

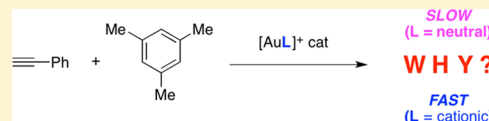
Understanding the Effect of α -Cationic Phosphines and Group 15 Analogues on π -Acid Catalysis

Yago García-Rodeja and Israel Fernández*[✉]

Departamento de Química Orgánica I, Facultad de Ciencias Químicas, Universidad Complutense, 28040 Madrid, Spain

Supporting Information

ABSTRACT: The factors responsible for the experimentally observed acceleration of π -acid-catalyzed reactions induced by α -cationic phosphines and group 15 analogues have been computationally explored within the density functional theory framework. To this end, the gold(I)-catalyzed hydroarylation reactions of phenylacetylene and mesitylene involving both neutral and cationic ligands (L) have been quantitatively analyzed in detail using the combination of the activation strain model of reactivity and the energy decomposition analysis methods. It is found that the activating effect of the cationic ligand finds its origin in the much stronger interaction between the deformed reactants along the entire reaction coordinate, which in turn derives from the much higher $\pi(\text{acetylene}) \rightarrow \sigma^*(\text{Au-L})$ interaction in the initially formed acetylene-gold(I) π -complex.

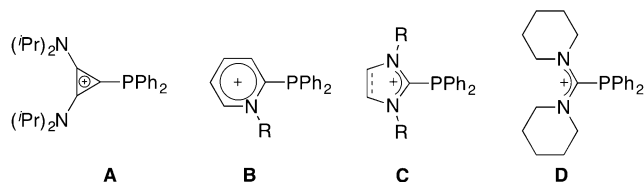


INTRODUCTION

The design and preparation of new ligands arguably play a key role in the development of known and new catalytic reactions. This is mainly due to the fact that ligands are crucial for controlling the reactivity and even the selectivity (from regio- or chemoselectivity to enantioselectivity) of transition metal catalyzed transformations.^{1,2} In this sense, α -cationic phosphines (and related arsines) have attracted considerable attention recently because the attachment of a positively charged moiety directly to the coordinating atom significantly increases the ability of these ligands to accept electronic density from the transition metal fragment.³ As a result, it was observed that these novel charged ligands lead to a significant enhancement of the activity of π -acid catalysts.

In this particular field of ligand development, Alcarazo and co-workers³ have prepared a series of monocationic phosphines containing cyclopropenium,⁴ pyridinium,⁵ imidazolium, or amidinium substituents⁶ (see Chart 1). The performance of

Chart 1. Representative α -Cationic Phosphines Prepared Experimentally



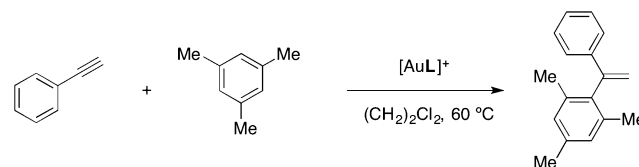
these ligands was tested in several catalytic processes requiring high Lewis acidity at the metal center such as gold(I)- or Pt(II)-catalyzed hydroarylation reactions. In general, it was found that these species are able to induce a significant acceleration of the process as compared to their neutral counterparts (i.e., PPh_3 or P(OPh)_3).

The enhanced catalytic activity induced by these cationic species has been qualitatively related to different electronic

properties of the ligands such as their Tolman electronic parameters (TEPs)⁷ and the corresponding oxidation potentials ($E_p(\text{ox})$).³ Whereas one should be cautious when using the former values, as the CO stretching frequencies do not unequivocally reflect the donicity of ancillary ligands,⁸ the latter values were suggested to be a more reliable parameter to rank the electronic properties (i.e., σ -donor/ π -acceptor ability) of the ligands. Despite that, the intrinsic physical factors governing the observed enhanced catalytic activity induced by this family of ligands are so far not fully understood.

On the other hand, the relatively recent introduction of the so-called activation strain model (ASM) of reactivity,⁹ in combination with the energy decomposition analysis (EDA) method,¹⁰ has allowed us to gain a deeper quantitative understanding of those factors controlling different fundamental processes in both organic (for instance, $\text{S}_{\text{N}}2$ and E2 reactions¹¹ and pericyclic reactions)¹² and organometallic transformations.¹³ For this reason, we decided herein to apply the combination of the ASM and EDA methods to assess the influence of these cationic ligands on π -acid catalysis in a quantitative way. To this end, we have selected the gold(I)-catalyzed hydroarylation reaction of phenylacetylene with mesitylene depicted in Scheme 1, which was also experimentally explored by Alcarazo and co-workers.⁵ In addition to α -cationic phosphines, the effect

Scheme 1. Gold(I)-Catalyzed Hydroarylation Reaction Considered in This Study



Received: November 16, 2016

of strongly related arsines (also prepared experimentally very recently)¹⁴ and unexplored group 15 analogues on the process shall be considered as well.

COMPUTATIONAL DETAILS

All the calculations reported in this paper were obtained with the GAUSSIAN 09 suite of programs.¹⁵ All reactants, transition structures, and reaction products were optimized using the B3LYP functional¹⁶ using the double- ζ quality def2-SVP basis sets¹⁷ for all atoms, which include a pseudopotential for gold. All stationary points were characterized by frequency calculations.¹⁸ Reactants and products have positive definite Hessian matrices, whereas transition structures (TSs) show only one negative eigenvalue in their diagonalized force constant matrices,¹⁹ and their associated eigenvectors were confirmed to correspond to the motion along the reaction coordinate under consideration using the intrinsic reaction coordinate (IRC) method.²⁰ Single-point calculations were performed to refine the computed energies on the optimized gas-phase geometries using the B3LYP functional in conjunction with the D3 dispersion correction suggested by Grimme et al.²¹ and the triple- ζ quality plus polarization def2-TZVP basis set¹⁷ for all atoms. Solvent effects (solvent = dichloroethane) were also taken into account in the single-point calculations using the polarizable continuum model (PCM).²² This level is thus denoted PCM(dichloroethane)-B3LYP-D3/def2-TZVP//B3LYP/def2-SVP.

Activation Strain Analyses of Reaction Profiles. The activation strain model of reactivity, also known as the *distortion/interaction model*,²³ is a fragment approach to understanding chemical reactions, in which the height of reaction barriers is described and understood in terms of the original reactants.⁹ Thus, the potential energy surface $\Delta E(\zeta)$ is decomposed, along the reaction coordinate ζ , into the strain $\Delta E_{\text{strain}}(\zeta)$ associated with deforming the individual reactants plus the actual interaction $\Delta E_{\text{int}}(\zeta)$ between the deformed reactants (eq 1):

$$\Delta E(\zeta) = \Delta E_{\text{strain}}(\zeta) + \Delta E_{\text{int}}(\zeta) \quad (1)$$

Herein, the reaction coordinate ζ is defined as the projection of the IRC on the forming C...C distance between the reactive carbon atom of the initially formed phenylacetylene-gold(I) π -complex and the carbon atom of mesitylene. This reaction coordinate ζ undergoes a well-defined change in the course of the reaction from ∞ to the equilibrium C...C distance in the corresponding transition structures.

The strain $\Delta E_{\text{strain}}(\zeta)$ is determined by the rigidity of the reactants and on the extent to which groups must reorganize in a particular reaction mechanism, whereas the interaction $\Delta E_{\text{int}}(\zeta)$ between the reactants depends on their electronic structure and on how they are mutually oriented as they approach each other. It is the interplay between $\Delta E_{\text{strain}}(\zeta)$ and $\Delta E_{\text{int}}(\zeta)$ that determines if and at which point along ζ a barrier arises, namely, at the point where $d\Delta E_{\text{strain}}(\zeta)/d\zeta = -d\Delta E_{\text{int}}(\zeta)/d\zeta$.

Furthermore, the interaction energy can be further decomposed by means of the so-called energy decomposition analysis¹⁰ method into the following meaningful terms (eq 2):

$$\Delta E_{\text{int}}(\zeta) = \Delta E_{\text{elstat}}(\zeta) + \Delta E_{\text{Pauli}}(\zeta) + \Delta E_{\text{orb}}(\zeta) + \Delta E_{\text{disp}}(\zeta) \quad (2)$$

The term ΔE_{elstat} corresponds to the classical electrostatic interaction between the unperturbed charge distributions of the deformed reactants and is usually attractive. The Pauli repulsion ΔE_{Pauli} comprises the destabilizing interactions between occupied orbitals and is responsible for any steric repulsion. The orbital interaction ΔE_{orb} accounts for electron-pair bonding, charge transfer (interaction between occupied orbitals on one moiety with unoccupied orbitals on the other, including HOMO–LUMO interactions), and polarization (empty-occupied orbital mixing on one fragment due to the presence of another fragment). Finally, the ΔE_{disp} term takes into account the interactions that are due to dispersion forces. The EDA calculations reported herein were carried out at the dispersion-corrected BP86²⁴-D3²¹ level in combination with the frozen core TZ2P²⁵ basis sets using the optimized B3LYP/def2-SVP geometries

with the ADF 2014 program package.²⁶ Scalar relativistic effects were incorporated by applying the zeroth-order regular approximation (ZORA).²⁷ This level is therefore denoted ZORA-BP86-D3/TZ2P//B3LYP/def2-SVP.

RESULTS AND DISCUSSION

The effect of the α -cationic substituent directly attached to the $-\text{PPh}_2$ moiety on the gold(I)-catalyzed hydroarylation reaction of phenylacetylene with mesitylene was studied first. As previously reported for strongly related processes,²⁸ this transformation involves the initial formation of a π -complex (readily formed upon coordination of the triple bond of phenylacetylene to the gold(I) catalyst) followed by the nucleophilic attack of mesitylene.²⁹ The final alkene is then produced through a Au–C bond protonolysis reaction, a process that is typically mediated by the counteranion present in the initial gold(I) precatalyst (Figure 1).²⁸ In most cases, the nucleophilic

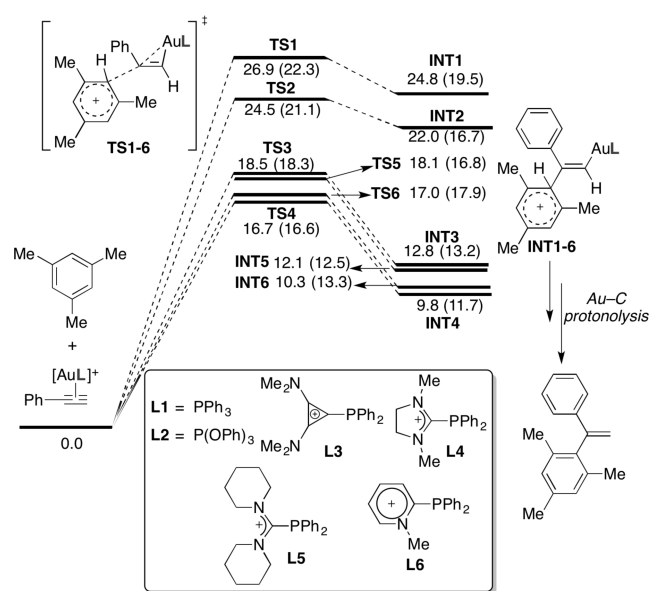


Figure 1. Computed reaction profile for the initial step of the studied gold(I)-catalyzed hydroarylation reaction between phenylacetylene and mesitylene. Relative free energies (computed at 298 K) are given in kcal/mol. Plain values refer to B3LYP/def2-SVP calculations, whereas values within parentheses were computed at the PCM(dichloroethane)-B3LYP-D3/def2-TZVP//B3LYP/def2-SVP level.

addition reaction constitutes the rate-limiting step of the entire transformation,²⁸ and for this reason, herein we only focused on this particular reaction step.

As readily seen in Figure 1, the replacement of the parent neutral ligand PPh_3 (L1) or P(OPh)_3 (L2) by a α -cationic phosphine (L3–L6) clearly leads to a remarkable decrease of the corresponding activation barrier (from 26.9 kcal/mol for L1 up to ca. 17.0 kcal/mol for L4 and L6), which nicely agrees with the acceleration induced by the α -cationic ligand experimentally observed. Furthermore, the computed endergonicity of the transformation systematically decreases in the presence of the cationic ligands L3–L6 as well.

Closer inspection of the optimized geometries of the corresponding transition states TS1–6 indicates that the α -cationic phosphine ligands L3–L6 lead to earlier transition states (i.e., the forming C...C distances become longer) than neutral ligands (see Figure 2). Interestingly, it is found that these late transition states are associated with higher activation

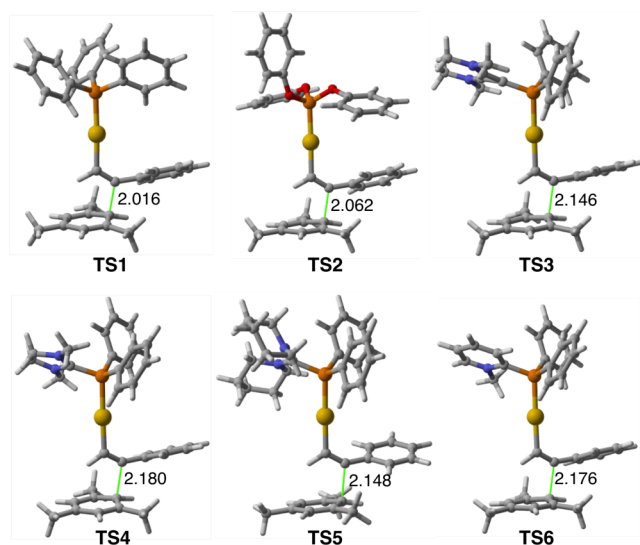


Figure 2. Fully optimized transition states TS1–6 associated with the C···C bond forming reaction in the considered gold(I)-hydroarylation reactions. Bond distances, computed at the B3LYP/def2-SVP level, are given in angstroms.

barriers and more endergonic transformations than earlier transition states. This finding, which nicely agrees with the Hammond–Leffer postulate,³⁰ becomes evident from the very good linear relationships (correlation coefficients $R^2 \approx 1.0$) observed when plotting the C···C bond forming distance in the transition states TS1–6 versus the corresponding computed reaction and activation energies (Figure 3).

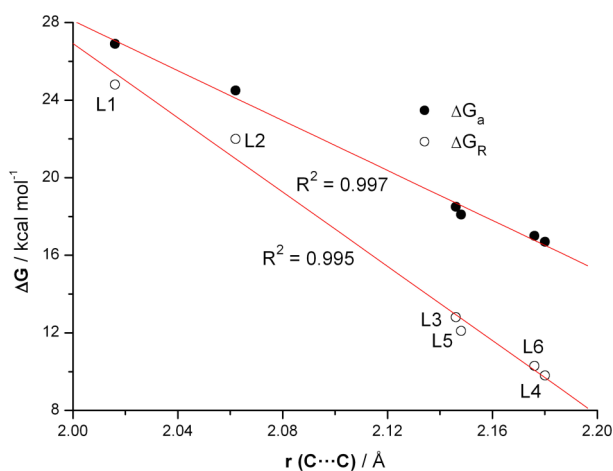


Figure 3. Plot of the computed activation (black circles) and reaction (white circles) energies versus the C···C bond forming distances of transition states TS1–6. All data have been computed at the B3LYP/def2-SVP level.

The activation strain model⁹ of reactivity was applied next to gain more quantitative insight into the physical factors controlling the observed acceleration of the process induced by the α -cationic ligand. To this end, we compared the process involving the parent neutral phosphine L1 (PPh₃) with the hydroarylation reaction involving the cationic pyridinium ligand L6. Figure 4 shows the computed activation strain diagrams (ASDs) for both transformations from the initial stages of the processes up to the corresponding transition states. Both reactions exhibit quite similar ASDs. Thus, in both cases the

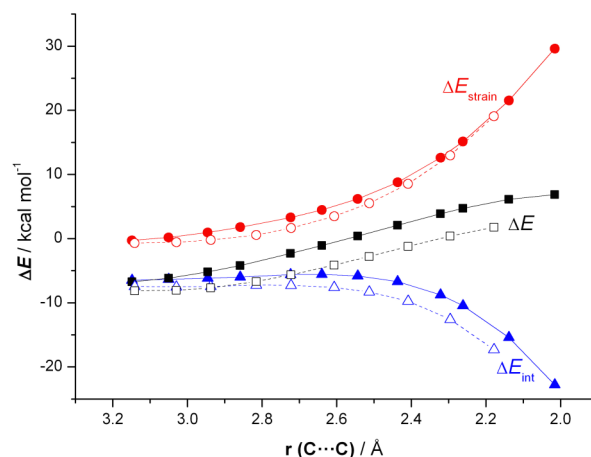


Figure 4. Comparative activation strain diagrams for the gold(I)-catalyzed hydroarylation reactions involving PPh₃ (L1, solid lines) and cationic L6 (dashed lines) as ligands along the reaction coordinate projected onto the forming C···C bond distance. All data have been computed at the PCM(dichloroethane)-B3LYP-D3/def2-TZVP//B3LYP/def2-SVP level.

interaction energy between the deformed reactants, measured by the ΔE_{int} term, remains nearly constant at the beginning of the reaction and then inverts at a certain point along the reaction coordinate (i.e., at forming C···C distances of ca. 2.5 Å), where it becomes more and more stabilizing as one approaches the corresponding transition-state region. At variance, the strain energy, measured by the ΔE_{strain} term, becomes more and more destabilizing from the initial stages of the reaction up to the transition state. Interestingly, the energy required to deform the reactants is nearly identical for both processes, particularly at the transition-state region where the height of the barrier is determined. For instance, at the same C···C bond forming distance of 2.2 Å, a value of $\Delta E_{\text{strain}} = 18.4$ kcal/mol was computed for the process involving PPh₃, whereas a rather similar value of $\Delta E_{\text{strain}} = 17.9$ kcal/mol was computed for the process involving L6 (Figure 4). Therefore, it can be safely concluded that the energy required to deform the reactants from their equilibrium geometries is not at all decisive for the observed enhanced reactivity of the catalyst bearing the α -cationic phosphine ligand.

In contrast, significant differences are observed when comparing the interaction energies between the deformed reactants. Indeed, the ΔE_{int} term is clearly more stabilizing for the process involving the cationic phosphine along the entire reaction coordinate. For instance, at the same C···C forming distance of 2.2 Å, a value of $\Delta E_{\text{int}} = -12.9$ kcal/mol was computed for the process involving PPh₃, whereas a higher value (i.e., more stabilizing) of $\Delta E_{\text{int}} = -16.5$ kcal/mol was computed for the process involving L6 (Figure 4). This stronger interaction between the deformed reactants from the very beginning of the transformation constitutes therefore the main factor controlling the lower activation barrier of the processes involving the α -cationic phosphines.

Further quantitative insight into the different contributions to the total interaction energy can be gained by means of the EDA method.¹⁰ As graphically shown in Figure 5, the orbital attractions between the deformed reactants (measured by the ΔE_{orb} term and dominated mainly by the π (mesitylene) $\rightarrow \pi^*$ (gold-complex) interaction) constitute the differential contribution when comparing the reactions involving the neutral

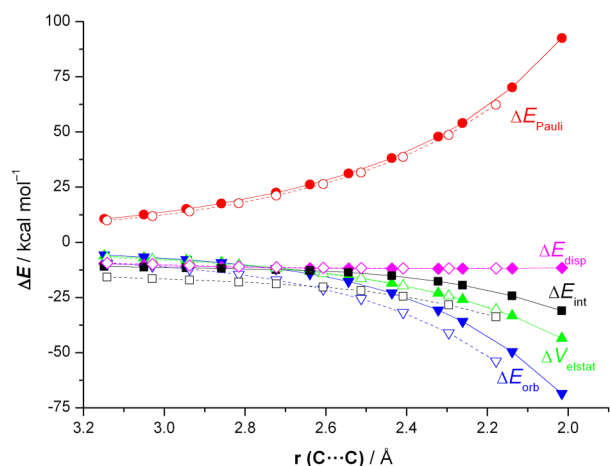


Figure 5. Decomposition of the interaction energy for the gold(I)-catalyzed hydroarylation reactions involving PPh_3 (L1, solid lines) and cationic L6 (dashed lines) as ligands along the reaction coordinate projected onto the forming $\text{C}\cdots\text{C}$ bond distance. All data have been computed at the ZORA-BP86-D3/TZ2P//B3LYP/def2-SVP level.

PPh_3 ligand and the cationic ligand L6 along the reaction coordinate. Thus, whereas the rest of the contributions (namely, Pauli repulsion and electrostatic and dispersion attractions) are practically identical for both transformations, the orbital term is clearly more stabilizing for the process involving L6. Indeed, the total interaction energy between the deformed reactants parallels the shape of the orbital interaction curve. For instance, at the same $\text{C}\cdots\text{C}$ forming distance of 2.2 Å, the difference between the orbital attractions for both processes $\Delta\Delta E_{\text{int}} = 8.7$ kcal/mol roughly matches the difference in the total interaction energy, $\Delta\Delta E_{\text{int}} = 10.8$ kcal/mol. Therefore, it can be concluded that the acceleration induced by the α -cationic phosphine ligand finds its origin mainly in the stronger orbital interaction between the reactants along the entire reaction coordinate.

The above finding strongly suggests that the α -cationic ligand significantly increases the π -acceptor ability of the initial acetylene-Au(I) complex. To quantitatively support this hypothesis, the main orbital contributions present in the different acetylene-Au(I) π -complexes considered in this study were analyzed by means of the NOCV (natural orbital for chemical valence) extension of the EDA method.³¹ Thus, the EDA-NOCV approach, which provides pairwise energy contributions for each pair of interacting orbitals to the total bond energy, indicates that two main molecular orbital interactions are present in the initially formed acetylene-Au(I) complexes, namely, the donation from the π -molecular orbital of the acetylene fragment to the vacant Au–P antibonding orbital of the $[\text{AuL}]^+$ moiety (denoted as ρ_1) and the back-donation (ρ_2) from a doubly occupied atomic orbital located at the transition metal to the π^* -molecular orbital of the acetylene fragment (see Figure 6 for $L = \text{PPh}_3$, charge flow is red \rightarrow blue).

Not surprisingly, the direct donation from the acetylene fragment is systematically much stronger than the back-donation interaction ($\Delta E(\rho_1) > \Delta E(\rho_2)$) regardless of the ligand L attached to the transition metal (Table 1). Moreover, whereas this back-donation remains almost constant for all species, the ρ_1 interaction strongly depends on the nature of the phosphine ligand. Indeed, this interaction becomes clearly much stronger for those complexes having α -cationic phosphine ligands in the order $\text{L1} < \text{L2} \ll \text{L3} < \text{L5} < \text{L4} \approx \text{L6}$, which, strikingly,

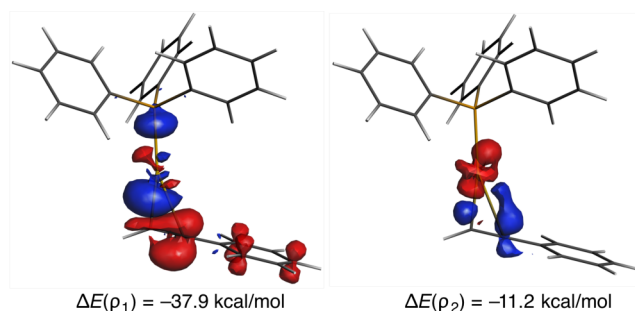


Figure 6. Plot of the deformation densities $\Delta\rho$ of the pairwise orbital interactions present in the $[(\text{Ph}_3\text{P})\text{Au}^+]$ -phenylacetylene complex and associated stabilization energies $\Delta E(\rho)$. The color code of the charge flow is red \rightarrow blue. Data computed at the ZORA-BP86-D3/TZ2P//B3LYP/def2-SVP level (isosurface value of 0.002 au).

Table 1. Computed NOCV Stabilization Energies $\Delta E(\rho)$ (in kcal/mol) Present in the Initial $[(L)\text{Au}^+]$ -Phenylacetylene Complexes^a

L	$\Delta E(\rho_1)$	$\Delta E(\rho_2)$	LUMO/eV	ΔG_a^{b}
L1	-37.9	-11.2	-6.40	26.9
L2	-44.4	-11.2	-6.82	24.5
L3	-55.5	-10.8	-8.94	18.5
L4	-59.9	-10.5	-9.25	16.7
L5	-56.3	-10.6	-9.04	18.1
L6	-59.2	-10.3	-9.45	17.0

^aAll data have been computed at the ZORA-BP86-D3/TZ2P//B3LYP/def2-SVP level. ^bActivation energies (in kcal/mol) were computed at the B3LYP/def2-SVP level.

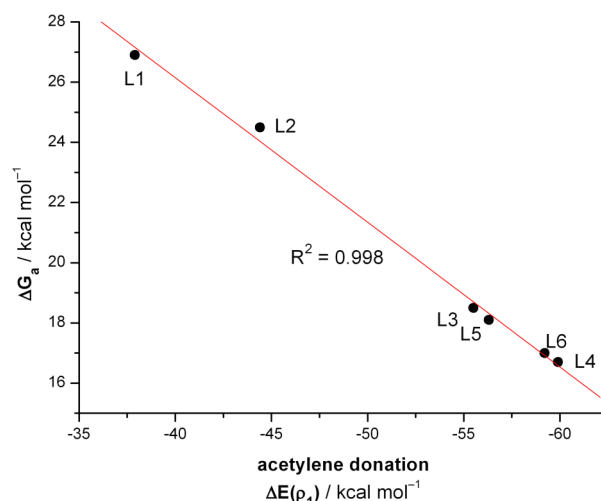


Figure 7. Plot of computed NOCV $\pi(\text{acetylene}) \rightarrow \sigma^*(\text{Au-P})$ interaction, $\Delta E(\rho_1)$, in the initial $[(L)\text{Au}^+]$ -phenylacetylene complexes versus the computed activation barriers (ΔG_a).

matches the computed activation barriers for the reactions involving these ligands. For this reason, a very good linear relationship (correlation coefficient of 0.998, Figure 7) was found when plotting the computed barriers versus the energies associated with the $\pi(\text{acetylene}) \rightarrow \sigma^*(\text{Au-P})$ interaction, $\Delta E(\rho_1)$, which, therefore, can be used as a reliable, quantitative measure of the activating effect of the ligand on this Au(I)-catalyzed hydroarylation reaction.

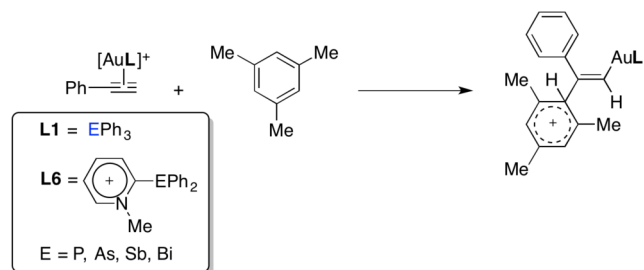
The existence of this linear correlation therefore indicates that the activation barrier of this type of transformations can

be easily predicted by simply computing the direct electronic donation in the initially formed π -complex, even for hitherto unknown ligands. Furthermore, from the data in Table 1, it becomes clear that the LUMO values of these complexes follow a similar trend to that of the $\Delta E(\rho_1)$ values and, therefore, may be used as well to assess the π -acceptor ability of these species, as previously suggested.^{3b} However, in view of the minor anomalies in the LUMO values observed when comparing ligands L4 and L6 (i.e., L6 leads to a slightly higher activation barrier even though the corresponding LUMO is more stabilized), the $\Delta E(\rho_1)$ values seem to be a more accurate parameter to quantify the effect of the ligand on the π -acceptor ability of the complex.

To complete this study, we also explored the effect of the group 15 coordinating atom present in the ligand L on π -acid catalysis. Quite recently, Alcarazo and co-workers prepared a series of α -cationic arsines, which were also found to increase the activity of π -acid catalysts in strongly related transformations.¹⁴ Thus, a similar acceleration to that observed when using phosphines was found in the Pt(II)-catalyzed cycloisomerization of enynes (leading to trisubstituted cyclopropanes) when replacing a phenyl group in the parent AsPh_3 ligand by an α -cationic substituent.

In order to understand the effect of the experimentally prepared arsenic ligands and make predictions about the influence of heavier group 15 analogues on this type of transformations, we focused again on the gold(I)-hydroarylation reaction involving phenylacetylene and mesitylene considered above by selecting the parent L1 (EPh_3 , E = P, As, Sb, and Bi) and cationic L6 ligands (i.e., having the methylpyridinium moiety, Scheme 2).

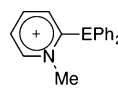
Scheme 2. Gold(I)-Catalyzed Hydroarylation Reactions Involving Group 15 Element Containing Ligands



From the data gathered in Table 2, it is clear that the involvement of a heavier group 15 atom in the ligand does not alter the scenario described above. Thus, the processes with the α -cationic ligand become kinetically more favorable and less endergonic than the corresponding transformations with the neutral EPh_3 ligand regardless of the group 15 E atom. Once again, it is found that the reactions involving the cationic L6 ligands proceed through earlier transition states ($\text{C}\cdots\text{C}$ forming distances in the range of 2.174–2.199 Å) than those processes involving the respective neutral ligands L1 (average $\text{C}\cdots\text{C}$ forming distances of 2.032 Å, see Figure S1 in the Supporting Information). Moreover, our calculations also predict that no significant further acceleration will be expected when replacing the phosphorus or arsenic atom by their heavier group 15 congeners in the reaction involving either neutral or cationic ligands (the computed activation barrier differences, $\Delta\Delta G_a$, are only ca. 1–2 kcal/mol; see Table 2).

We have also applied the ASM approach to confirm that the lower activation barrier computed for the processes involving

Table 2. Computed Free Activation (ΔG_a) and Reaction (ΔG_R) Energies (in kcal/mol) for the Gold(I)-Catalyzed Hydroarylation Reaction Involving Ligands L1 and L6^a

	EPh_3 L1		 L6	
E	ΔG_a	ΔG_R	ΔG_a	ΔG_R
P	26.9 (22.3)	24.8 (19.5)	17.0 (17.9)	10.3 (13.3)
As	28.9 (21.9)	24.2 (18.6)	19.6 (17.6)	10.1 (12.9)
Sb	28.9 (22.0)	24.8 (18.7)	19.5 (17.4)	10.3 (12.8)
Bi	27.2 (20.7)	23.1 (17.0)	17.8 (16.5)	10.6 (11.0)

^aPlain values refer to B3LYP/def2-SVP calculations, whereas values within parentheses were computed at the PCM(dichloroethane)-B3LYP-D3/def2-TZVP//B3LYP/def2-SVP level.

the group 15 element containing L6 ligands finds its origin also in the stronger interactions between the deformed reactants along the entire reaction coordinate. To this end, we selected the hydroarylation reaction involving SbPh_3 and its corresponding pyridinium ligand L6. As readily seen in Figure 8, it is

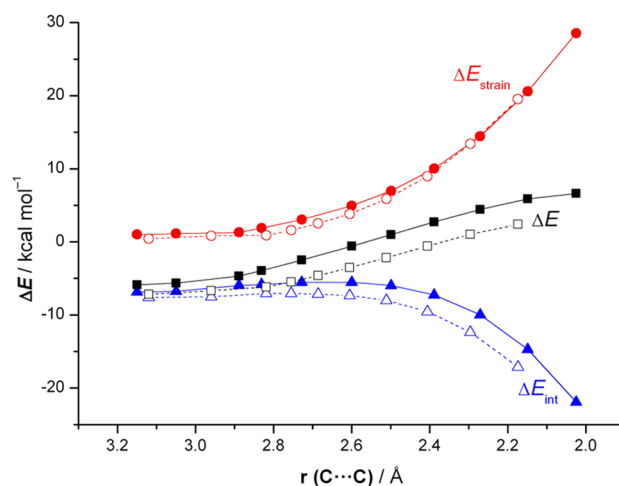


Figure 8. Comparative activation strain diagrams for the gold(I)-catalyzed hydroarylation reactions involving SbPh_3 (L1, solid lines) and cationic L6-Sb (dashed lines) as ligands along the reaction coordinate projected onto the forming $\text{C}\cdots\text{C}$ bond distance. All data have been computed at the PCM(dichloroethane)-B3LYP-D3/def2-TZVP//B3LYP/def2-SVP level.

confirmed that the strain energy is not at all responsible for the computed different barrier energies since the ΔE_{strain} curves for both processes are nearly identical along the entire reaction coordinate. Once again, the stronger interaction between the deformed reactants computed for the entire pathway involving the cationic ligand constitutes the differential decisive factor responsible for the acceleration of this transformation. As expected, this stronger interaction can be ascribed to the much higher π -acceptor ability of the corresponding initial gold(I)-acetylene π -complex. This is again reflected in the much higher NOCV- $\Delta E(\rho_1)$ value (i.e., donation from the acetylene to the gold(I) moiety) computed for the π -complex having the L6-Sb ligand as compared to the neutral L1 (SbPh_3) ligand (Figure 9).

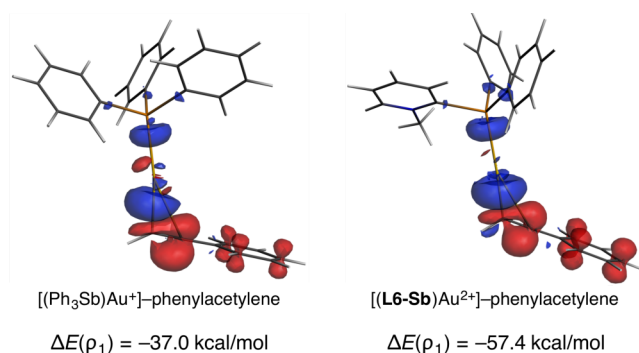


Figure 9. Plot of the deformation densities $\Delta\rho$ of the pairwise orbital interactions present in the $[(\text{Ph}_3\text{Sb})\text{Au}^+]$ -phenylacetylene (left) and $[(\text{L6-Sb})\text{Au}^{2+}]$ -phenylacetylene (right) complexes and corresponding associated stabilization energies $\Delta E(\rho_1)$. The color code of the charge flow is red \rightarrow blue. Data computed at the ZORA-BP86-D3/TZ2P//B3LYP/def2-SVP level (isosurface value of 0.002 au).

CONCLUSIONS

From the computational study reported herein, the following conclusions can be drawn: (i) the replacement of a phenyl group in the EPh_3 ($\text{E} =$ group 15 atom) ligand by a α -cationic substituent leads to a remarkable acceleration (i.e., a lower activation barrier) of the initial step of the gold(I)-hydroarylation reaction involving phenylacetylene and mesitylene. (ii) In addition, the transformation becomes less endergonic when the cationic ligand is present. (iii) Both parameters (i.e., activation and reaction energies) nicely correlate with the computed $\text{C}\cdots\text{C}$ bond forming distance in the corresponding transition states in the sense that earlier transition structures are associated with lower activation and reaction energies (therefore satisfying the Hammond–Leffer postulate). (iv) The activating effect of the cationic ligand finds its origin in the computed much stronger interaction between the deformed reactants along the entire reaction coordinate as compared to the process involving neutral (PPh_3 or $\text{P}(\text{OPh})_3$) ligands. (v) This is almost exclusively due to the much stronger orbital interactions between these deformed reactants in the α -cationic pathway, which in turn derive from the much stronger $\pi(\text{acetylene}) \rightarrow \sigma^*(\text{Au-P})$ interaction in the initially formed acetylene-gold(I) π -complex. (vi) Similar conclusions can be drawn when considering heavier group 15 elements as coordinating atoms. Despite that, our calculations predict that no significant further acceleration will be expected when replacing the phosphorus or arsenic atom by their heavier group 15 congeners in the ligands.

ASSOCIATED CONTENT

Supporting Information

The Supporting Information is available free of charge on the ACS Publications website at DOI: 10.1021/acs.organomet.6b00859.

Figure S1, Cartesian coordinates (in Å), and total free energies (in au) of all the stationary points discussed in the text (PDF)

Optimized structure (XYZ)

AUTHOR INFORMATION

Corresponding Author

*E-mail (I. Fernández): israel@quim.ucm.es.

ORCID

Israel Fernández: 0000-0002-0186-9774

Notes

The authors declare no competing financial interest.

ACKNOWLEDGMENTS

Financial support was provided by the Spanish Ministerio de Economía y Competitividad (MINECO) and FEDER (Projects CTQ2013-44303-P and CTQ2014-51912-REDC). Y.G.-R. acknowledges the MINECO for a FPI grant.

REFERENCES

- (1) (a) Engle, K. M.; Yu, J.-Q. *J. Org. Chem.* **2013**, *78*, 8927–8955. (b) Hansen, E. C.; Pedro, D. J.; Wotal, A. C.; Gower, N. J.; Nelson, J. D.; Caron, S.; Weix, D. J. *Nat. Chem.* **2016**, *8*, 1126–1130.
- (2) For a recent review on computational studies highlighting the effect of ligands on homogenous catalysis, see: Sperger, T.; Sanhueza, I. A.; Kalvet, I.; Schoenebeck, F. *Chem. Rev.* **2015**, *115*, 9532–9586.
- (3) For recent reviews, see: (a) Alcarazo, M. *Chem. - Eur. J.* **2014**, *20*, 7868–7877. (b) Alcarazo, M. *Acc. Chem. Res.* **2016**, *49*, 1797–1805.
- (4) Petušková, J.; Bruns, H.; Alcarazo, M. *Angew. Chem., Int. Ed.* **2011**, *50*, 3799–3802. (b) Petušková, J.; Patil, M.; Holle, S.; Lehmann, C. W.; Thiel, W.; Alcarazo, M. *J. Am. Chem. Soc.* **2011**, *133*, 20758–20760.
- (5) Tinnermann, H.; Wille, C.; Alcarazo, M. *Angew. Chem., Int. Ed.* **2014**, *53*, 8732–8736.
- (6) Haldón, E.; Kozma, A.; Tinnermann, H.; Gu, L.; Goddard, R.; Alcarazo, M. *Dalton Trans.* **2016**, *45*, 1872–1876.
- (7) Tolman, C. A. *Chem. Rev.* **1977**, *77*, 313–348.
- (8) See for instance: Valyaev, D. A.; Brousses, R.; Lugan, N.; Fernández, I.; Sierra, M. A. *Chem. - Eur. J.* **2011**, *17*, 6602–6605.
- (9) (a) Bickelhaupt, F. M. *J. Comput. Chem.* **1999**, *20*, 114–128. For reviews, see: (b) Fernández, I.; Bickelhaupt, F. M. *Chem. Soc. Rev.* **2014**, *43*, 4953–4967. (c) Fernández, I. *Phys. Chem. Chem. Phys.* **2014**, *16*, 7662. (d) Wolters, L. P.; Bickelhaupt, F. M. *WIREs Comput. Mol. Sci.* **2015**, *5*, 324–343. See also: (e) Fernández, I. In *Discovering the Future of Molecular Sciences*; Pignataro, B., Ed.; Wiley-VCH: Weinheim, 2014; pp 165–187.
- (10) (a) Morokuma, K. *J. Chem. Phys.* **1971**, *55*, 1236–1244. For recent reviews, see: (b) von Hopffgarten, M.; Frenking, G. *WIREs Comput. Mol. Sci.* **2012**, *2*, 43–62. (c) Frenking, G.; Bickelhaupt, F. M. The EDA Perspective of Chemical Bonding. In *The Chemical Bond—Fundamental Aspects of Chemical Bonding*; Frenking, G.; Shaik, S., Eds.; Wiley-VCH: Weinheim, 2014; pp 121–158.
- (11) (a) van Bochove, M. A.; Swart, M.; Bickelhaupt, F. M. *J. Am. Chem. Soc.* **2006**, *128*, 10738–10744. (b) Bento, A. P.; Bickelhaupt, F. M. *J. Org. Chem.* **2007**, *72*, 2201–2207. (c) Bento, A. P.; Bickelhaupt, F. M. *J. Org. Chem.* **2008**, *73*, 7290–7299. (d) Fernández, I.; Frenking, G.; Uggerud, E. *Chem. - Eur. J.* **2009**, *15*, 2166–2175. (e) Fernández, I.; Frenking, G.; Uggerud, E. *J. Org. Chem.* **2010**, *75*, 2971–2980. (f) Fernández, I.; Bickelhaupt, F. M.; Uggerud, E. *J. Org. Chem.* **2013**, *78*, 8574–8584. (g) Wolters, L. P.; Ren, Y.; Bickelhaupt, F. M. *ChemistryOpen* **2014**, *3*, 29–36.
- (12) (a) Fernández, I.; Bickelhaupt, F. M.; Cossío, F. P. *Chem. - Eur. J.* **2009**, *15*, 13022–13032. (b) Fernández, I.; Cossío, F. P.; Bickelhaupt, F. M. *J. Org. Chem.* **2011**, *76*, 2310–2314. (c) Fernández, I.; Bickelhaupt, F. M.; Cossío, F. P. *Chem. - Eur. J.* **2012**, *18*, 12395–12403. (d) Nieto Faza, O.; Silva López, C.; Fernández, I. *J. Org. Chem.* **2013**, *78*, 5669–5676. (e) Hong, X.; Liang, Y.; Houk, K. N. *J. Am. Chem. Soc.* **2014**, *136*, 2017–2025. (f) Fernández, I.; Bickelhaupt, F. M.; Cossío, F. P. *Chem. - Eur. J.* **2014**, *20*, 10791–10801. (g) Fernández, I.; Cossío, F. P. *J. Comput. Chem.* **2016**, *37*, 1265–1273. (h) García-Rodeja, Y.; Fernández, I. *J. Org. Chem.* **2016**, *81*, 6554–6562. (i) García-Rodeja, Y.; Solà, M.; Fernández, I. *Chem. - Eur. J.* **2016**, *22*, 10572–10580.
- (13) (a) van Zeist, W.-J.; Bickelhaupt, F. M. *Dalton Trans.* **2011**, *40*, 3028–3038. (b) Wolters, L. P.; Bickelhaupt, F. M. *ChemistryOpen* **2013**, *2*, 106–114. (c) Green, A. G.; Liu, P.; Merlic, C. A.; Houk, K. N. *J. Am. Chem. Soc.* **2014**, *136*, 4575–4583. (d) Fernández, I.; Wolters, L. P.; Bickelhaupt, F. M. *J. Comput. Chem.* **2014**, *35*, 2140–2145.

- (e) Sosa Carrizo, E. D.; Bickelhaupt, F. M.; Fernández, I. *Chem. - Eur. J.* **2015**, *21*, 14362–14369. (f) García-Rodeja, Y.; Bickelhaupt, F. M.; Fernández, I. *Chem. - Eur. J.* **2016**, *22*, 13669–13676.
- (14) Dube, J. W.; Zheng, Y.; Thiel, W.; Alcarazo, M. *J. Am. Chem. Soc.* **2016**, *138*, 6869–6877.
- (15) Frisch, M. J.; Trucks, G. W.; Schlegel, H. B.; Scuseria, G. E.; Robb, M. A.; Cheeseman, J. R.; Scalmani, G.; Barone, V.; Mennucci, B.; Petersson, G. A.; Nakatsuji, H.; Caricato, M.; Li, X.; Hratchian, H. P.; Izmaylov, A. F.; Bloino, J.; Zheng, G.; Sonnenberg, J. L.; Hada, M.; Ehara, M.; Toyota, K.; Fukuda, R.; Hasegawa, J.; Ishida, M.; Nakajima, T.; Honda, Y.; Kitao, O.; Nakai, H.; Vreven, T.; Montgomery, J. A., Jr.; Peralta, J. E.; Ogliaro, F.; Bearpark, M.; Heyd, J. J.; Brothers, E.; Kudin, K. N.; Staroverov, V. N.; Kobayashi, R.; Normand, J.; Raghavachari, K.; Rendell, A.; Burant, J. C.; Iyengar, S. S.; Tomasi, J.; Cossi, M.; Rega, N.; Millam, J. M.; Klene, M.; Knox, J. E.; Cross, J. B.; Bakken, V.; Adamo, C.; Jaramillo, J.; Gomperts, R.; Stratmann, R. E.; Yazyev, O.; Austin, A. J.; Cammi, R.; Pomelli, C.; Ochterski, J. W.; Martin, R. L.; Morokuma, K.; Zakrzewski, V. G.; Voth, G. A.; Salvador, P.; Dannenberg, J. J.; Dapprich, S.; Daniels, A. D.; Farkas, Ö.; Foresman, J. B.; Ortiz, J. V.; Cioslowski, J.; Fox, D. J. *Gaussian 09*, Revision D.01; Gaussian, Inc.: Wallingford, CT, 2009.
- (16) (a) Becke, A. D. *J. Chem. Phys.* **1993**, *98*, 5648–5652. (b) Lee, C.; Yang, W.; Parr, R. G. *Phys. Rev. B: Condens. Matter Mater. Phys.* **1998**, *37*, 785–789. (c) Vosko, S. H.; Wilk, L.; Nusair, M. *Can. J. Phys.* **1980**, *58*, 1200–1211.
- (17) Weigend, F.; Ahlrichs, R. *Phys. Chem. Chem. Phys.* **2005**, *7*, 3297–3305.
- (18) McIver, J. W.; Komornicki, A. K. *J. Am. Chem. Soc.* **1972**, *94*, 2625–2633.
- (19) Some transition states, particularly those containing heavy group 15 elements, presented an additional very low imaginary mode ($<-5\text{ cm}^{-1}$), which disappears when using a higher integration grid (keyword grid = SuperFineGrid).
- (20) González, C.; Schlegel, H. B. *J. Phys. Chem.* **1990**, *94*, 5523–5527.
- (21) Grimme, S.; Antony, J.; Ehrlich, S.; Krieg, H. *J. Chem. Phys.* **2010**, *132*, 154104–154119.
- (22) (a) Miertuš, S.; Scrocco, E.; Tomasi, J. *Chem. Phys.* **1981**, *55*, 117–129. (b) Pascual-Ahuir, J. L.; Silla, E.; Tuñón, I. *J. Comput. Chem.* **1994**, *15*, 1127–1138. (c) Barone, V.; Cossi, M. *J. Phys. Chem. A* **1998**, *102*, 1995–2001.
- (23) (a) Ess, D. H.; Houk, K. N. *J. Am. Chem. Soc.* **2007**, *129*, 10646–10647. (b) Ess, D. H.; Houk, K. N. *J. Am. Chem. Soc.* **2008**, *130*, 10187–10198. (c) Ess, D. H.; Jones, G. O.; Houk, K. N. *Org. Lett.* **2008**, *10*, 1633–1636. For relevant studies on other pericyclic reactions by Houk's group, see: (d) Schoenebeck, F.; Ess, D. H.; Jones, G. O.; Houk, K. N. *J. Am. Chem. Soc.* **2009**, *131*, 8121–8133. (e) Xu, L.; Doubleday, C. E.; Houk, K. N. *J. Am. Chem. Soc.* **2010**, *132*, 3029–3037. (f) Krenske, E. H.; Houk, K. N.; Holmes, A. B.; Thompson, J. *Tetrahedron Lett.* **2011**, *52*, 2181–2183.
- (24) Becke, A. D. *Phys. Rev. A: At., Mol., Opt. Phys.* **1988**, *38*, 3098–3100. (b) Perdew, J. P. *Phys. Rev. B: Condens. Matter Mater. Phys.* **1986**, *33*, 8822–8824.
- (25) (a) Snijders, J. G.; Baerends, E. J.; Vernooijs, P. *At. Data Nucl. Data Tables* **1981**, *26*, 483–574. (b) Krijn, J.; Baerends, E. J. *Fit Functions in the HFS-Method*, Internal Report (in Dutch); Vrije Universiteit Amsterdam: The Netherlands, 1984.
- (26) ADF, SCM; Theoretical Chemistry; Vrije Universiteit: Amsterdam, The Netherlands, <http://www.scm.com>.
- (27) (a) van Lenthe, E.; Baerends, E. J.; Snijders, J. G. *J. Chem. Phys.* **1993**, *99*, 4597–4610. (b) van Lenthe, E.; Baerends, E. J.; Snijders, J. G. *J. Chem. Phys.* **1994**, *101*, 9783–9792. (c) van Lenthe, E.; Ehlers, A.; Baerends, E. J. *J. Chem. Phys.* **1999**, *110*, 8943–8953.
- (28) See, for instance: (a) Alcaide, B.; Almendros, P.; Fernández, I.; Martín-Montero, R.; Martínez-Peña, F.; Ruiz, M. P.; Torres, M. R. *ACS Catal.* **2015**, *5*, 4842–4845. See also: (b) Soriano, E.; Fernández, I. *Chem. Soc. Rev.* **2014**, *43*, 3041–3105.
- (29) For other related recent studies on gold(I)-catalyzed reactions involving alkynes, see, for instance: (a) Hashmi, A. S. K. *Acc. Chem. Res.* **2014**, *47*, 864–876. (b) Pflästerer, D.; Hashmi, S. K. *Chem. Soc. Rev.* **2016**, *45*, 1331–1367. (c) Asiri, A. M.; Hashmi, A. S. K. *Chem. Soc. Rev.* **2016**, *45*, 4471–4503.
- (30) Hammond, G. S. *J. Am. Chem. Soc.* **1955**, *77*, 334–338.
- (31) Mitoraj, M. P.; Michalak, A.; Ziegler, T. *J. Chem. Theory Comput.* **2009**, *5*, 962–975.